ELSEVIER

Journal of Molecular Catalysis A: Chemical 117 (1997) 299–309

JOURNAL OF MOLECULAR CATALYSIS A: CHEMICAL

Kinetics and mechanism of the cobaloxime(II) catalyzed oxidative dehydrogenation and double bond cleavage of 3,3′,5,5′-tetra-*tert*-butyl-4,4′-dihydroxystilbene by O_2

László I. Simándi *, Tatiana L. Simándi

Central Research Institute for Chemistry of the Hungarian Academy of Sciences, P.O. Box 17, H-1525 Budapest, Hungary

Received 19 April 1996; accepted 1 July 1996

Abstract

In the presence of the cobaloxime(II) catalyst $[Co(Hdmg)_2(Ph_3P)_2]$, at room temperature and 1 atm O_2 or air, the dihydroxystilbene derivative referred to in the title (H_2StQ) undergoes oxidative dehydrogenation to the corresponding stilbenequinone (StQ), and parallel oxidative cleavage at the C=C double bond to afford 2,6-di-*tert*-butyl-4-hydroxybenzaldehyde (Ald). The two products are formed via a common anion radical intermediate stable enough for detection by ESR spectroscopy. A detailed kinetic analysis has been carried out by volumetric, spectrophotometric and HPLC techniques. The observed kinetic behavior is consistent with the formation of a superoxocobaloxime(III) intermediate, which generates the free radical intermediate from H_2StQ. In the steady state, the catalyst is present in a hydroxo-cobaloxime(III) precursor state, from which it is released via reduction to cobaloxime(II) by the anion radical.

Keywords: Cobaloxime(II); Oxidative dehydrogenation; Oxidative cleavage; Dihydroxystilbene cleavage; O_2 activation

1. Introduction

The activation of dioxygen by metal complexes has been attracting interest because of its relevance to biological oxidation and possible applications in environmentally acceptable technologies [1–4].

The role of transition metal dioxygen complexes as intermediates in various types of biomimetic homogeneous catalytic oxidations has been demonstrated in mechanistic studies, and functional metalloenzyme models have been designed [1,5]. Recently, attention has been focused on the role of free radicals in metalloenzymes [6,7]. Of particular interest are tyrosyl radicals in the active site of galactose oxidase [8,9] and ribonucleotide reductase [10].

We have studied the catalytic activation of dioxygen by cobaloxime(II) as well as some other macrocyclic cobalt(II) and manganese(II) complexes, primarily using aromatic phenol, thiophenol and aniline derivatives as model substrates [11–19]. In the cases investigated, these substrates undergo oxidative dehydrogenation to quinones, disulfides and quinoneimines with subsequent formation of heterocycles like 2,3-diaminophenazine or 2-aminophenoxazine-3-one [11–19]. Our recent kinetic work on the

* Corresponding author.

PII S1381-1169(96)00269-5

cobaloxime(II)-catalyzed oxidation of 2-aminophenol [20,21] has led to a functional model of phenoxazinone synthase involving free radical intermediates. In studies on the catalytic oxidative dehydrogenation of 3,5-di-*tert*-butylcatechol [22] free and coordinated anion radicals have been detected as intermediates, and a new catecholatocobaloxime(III) species capable of homolytic Co–O bond cleavage via low-energy ligand to metal electron transfer has been isolated and characterized. The observed behavior was interpreted in terms of a functional model for catecholase activity involving free radical intermediates.

In a search for further biomimetic oxidations in which relatively stable free radicals are expected to form, our attention turned toward stilbenequinone derivatives. The latter are known to react with peroxyl radicals, being thereby converted to stable free radicals [23]. Also, they are structurally related to the monomeric building blocks of lignin, viz. coumaryl, sinapyl and coniferyl alcohol, which undergo polymerization via phenoxyl type free radicals during the biosynthesis of lignin by laccase or peroxidases [6,24]. Similar free radicals are believed to play a role in the degradation of lignin by ligninases [25,26] or O_2 and alkali [27].

Free radicals have been postulated in the catalytic cleavage of the lignin models isoeugenol [28–30] and some stilbenols [31] with O_2 and cobalt(II) Schiff base complexes, but no direct evidence has been provided for their involvement. Alkenylphenols were found to undergo cleavage via a free radical [32].

A substrate which seemed likely to produce a stable free radical upon H-atom abstraction was 3,3′,5,5′-tetra-*tert*-butyl-4,4′-dihydroxystilbene (H_2StQ). Our previous work on the catalytic oxidation of 2-aminophenol in the presence of cobaloxime(II) derivatives [20,21] and on the reaction of 3,3′,5,5′-tetra-*tert*-butylstilbene-4,4′-quinone (StQ) with alkyl and phenyl radicals [23] indicated that it could form a phenoxyl type free radical in the presence of a cobaloxime(II) catalyst and dioxygen. The identification of free radical intermediates during the catalytic reaction provides important information to be utilized when constructing a suitable reaction mechanism.

We have found that in the presence of $[Co(Hdmg)_2(Ph_3P)_2]$ as catalyst H_2StQ is oxidized by dioxygen to StQ and 2,6-di-*tert*-butyl-4-hydroxybenzaldehyde (Ald), corresponding to symmetrical double bond cleavage. Upon dissolution in benzene this complex is known to become 5-coordinate by losing one of its Ph_3P ligands [33]. The results are described in this paper.

2. Experimental

Bis(dimethylglyoximato)cobalt(II) complexes were synthesized by the procedure reported in the literature [34].

StQ was synthesized as described earlier [23]. H_2StQ was prepared from StQ by reduction with Zn/glacial acetic acid (mp 242–243°C; lit. 244°C [36]). Ald was separated from the reaction mixture by evaporation and identified by infrared and ^{1}H NMR spectra [36] (mp 188–189°C; lit. 188°C [36]).

The catalytic reaction was carried out in benzene solution at substrate to catalyst ratios of ca. 10. Monitoring was done by gas volumetry, spectrophotometry and HPLC.

Rates of dioxygen uptake were measured in a constant pressure gas-volumetric apparatus. To start the reaction, the solid cobaloxime(II) catalyst was added to an intensively stirred, thermally equilibrated benzene solution of the H_2StQ substrate from a sample holder manipulated from the outside. The volume of absorbed O_2 was read periodically, using a gas burette. The rate of O_2 absorption was independent of the stirring rate, excluding eventual diffusion control effects.

IR spectra in KBr pellets were recorded on a Specord 75 spectrometer and ESR spectra on a JES-FE-3X spectrometer. UV–vis spectroscopic

measurements were done on a Hewlett-Packard 8452A diode array spectrophotometer.

HPLC analyses were performed on a Waters 991 system with a diode array detector (silica column, Spherisorb 5μ, eluent methanol:water = 90:10; elution rate 1.2 mL/min). Detection of Ald at 300 nm (R_f = 3 min), H_2StQ at 320 nm (R_f = 14.5 min), StQ at 450 nm (R_f = 25 min). Calibration with 4–5 samples of different masses was reproducible within about 1%. Samples withdrawn from the reacting mixture for HPLC analysis were quenched by 21-fold dilution with MeOH before injection.

3. Results and discussion

3.1. Stoichiometry

We have observed that in the presence of $[Co(Hdmg)_2(Ph_3P)_2]$ as catalyst H_2StQ undergoes catalytic oxidation to StQ and Ald in benzene or MeOH as solvent at room temperature and 1 bar of total air or dioxygen pressure. In the absence of catalyst the oxidation of H_2StQ cannot be detected under the same conditions.

In order to determine the stoichiometry, the oxidation was monitored by HPLC in the presence of the cobaloxime(II) catalyst. The variation of the concentrations of H_2StQ, StQ and Ald in time is shown in Fig. 1. No other materials could be detected in the reacting mixtures by HPLC or TLC.

The rates of H_2StQ consumption and product formation have been determined from similar curves measured at various conditions. The results are shown in Table 1.

The concentration profiles of H_2StQ and StQ exhibit a break at about t = 10 min, where a steady state is reached. The results reveal two major features:

(i) The mass balance for the substrate is fairly good, as demonstrated by the fact that the equation

$$[H_2StQ]_0 = [H_2StQ] + [StQ] + 0.5[Ald]$$

is fulfilled to within ±5% throughout 3 parallel runs.

(ii) The rates obtained by linear least-squares fits of the steady state sections after the break show that the equation

$$-d[H_2StQ]/dt = d[StQ]/dt + 0.5d[Ald]/dt$$

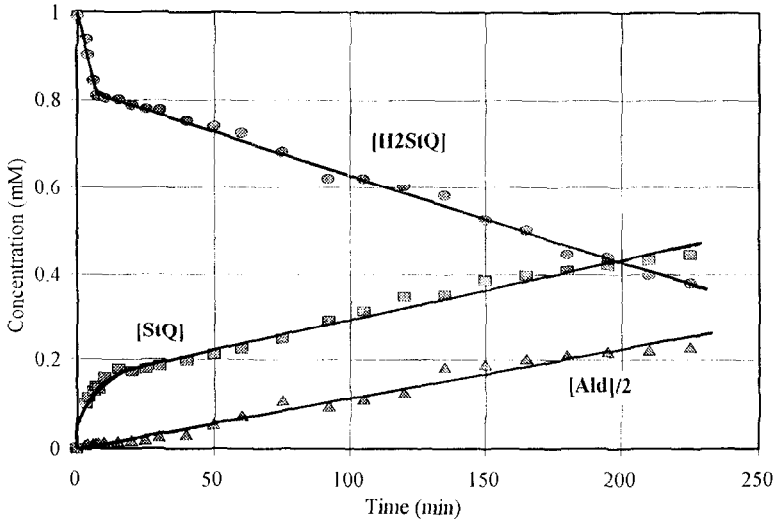

Fig. 1. Variation of the reactant and product concentrations with time. $[Co]_0$ = 0.145 mM; $[H_2StQ]_0$ = 0.991 mM; solvent: benzene; t = 25°C; 1 atm of air.

Table 1
Rates of substrate consumption and product formation in the steady state measured by HPLC and spectrophotometry

No.	Method	$[Co]_0$ (mM)	$[H_2StQ]_0$ (mM)	Rate of H_2StQ consumption (10^{-8} M s^{-1})	Rate of StQ formation (10^{-8} M s^{-1})	Rate of Ald formation (10^{-8} M s^{-1})	Time interval (min)
1	HPLC [a]	0.125	0.975	3.43	2.25	3.17	10–320
2	HPLC [b]	0.145	1.180	4.25	2.67	3.04	10–200
3	HPLC [c]	0.160	1.067	3.92	2.43	3.50	10–70
4	spectrophotometry [d]	0.140	0.989	3.57	2.10	2.67	10–200

Reaction mixture in benzene diluted before analysis with MeOH by factors of 11 [a], 21 [b], 41 [c] and 51 [d].

holds within about ±8% (3 runs), which is in agreement with the satisfactory mass balance.

The reaction was also monitored by recording the successive UV–vis spectra of the reaction mixture at various time intervals. The reaction was stopped by 51-fold dilution with MeOH and then scanned in the spectrophotometric cell, so each spectrum represents a separate run. The variation of the spectrum with time is displayed in Fig. 2. The presence of an isosbestic point (356 nm) shows that the reactant is transformed to the two products in two competitive reactions. A second, less well defined isosbestic point is present at ca. 290 nm.

Based on these data, the stoichiometry of oxidation of H_2StQ can be written as the combination of the two stoichiometric equations shown in Scheme 1.

The relative contribution of these two stoichiometries depends on the degree of H_2StQ conversion. According to Fig. 1, H_2StQ is initially transformed mainly to StQ, and Ald is formed much more slowly. In the steady state the relative rate of formation of StQ and Ald is approximately constant throughout a given run, indicating that they are formed in competitive reactions, via a common intermediate.

3.2. Free-radical intermediate

In a search of free-radical intermediates, we monitored the reaction by ESR spectroscopy. Although both cobaloxime(II) and superoxocobaloxime(III) derivatives are known to be paramagnetic and ESR-active under ambient conditions [34,35,37], their ESR spectra could

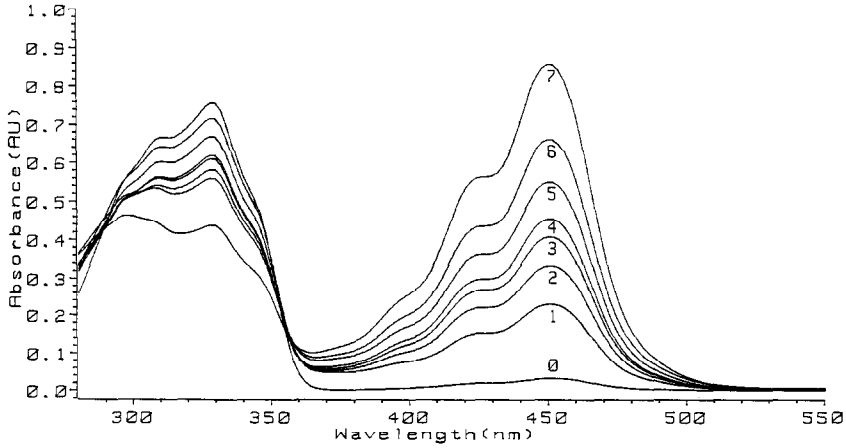

Fig. 2. Successive UV–vis spectra for the cobaloxime(II) catalyzed oxidation of H_2StQ. $[Co]_0 = 0.145$ mM; $[H_2StQ]_0 = 0.989$ mM; solvent: benzene; $t = 25$°C; 1 atm of air. Spectra were recorded for separate runs quenched by 51-fold dilution with MeOH. Reaction times: 0 (0), 3 (1), 17 (2), 45 (3), 60 (4), 90 (5), 120 (6) and 195 min (7).

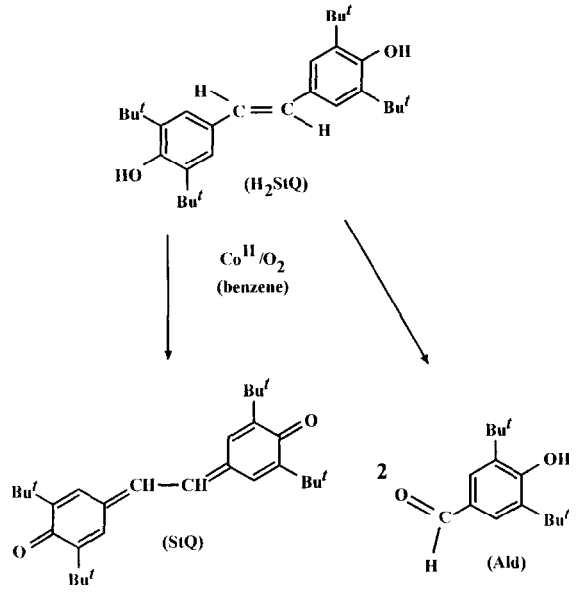

Scheme 1.

not be observed during the catalytic oxidation. This indicates that the cobaloxime added is present in the form of an ESR-silent cobaloxime(III) derivative, most likely $Co^{III}OH$ (see mechanism).

We have however observed the ESR spectrum shown in Fig. 3. By means of numerical simulation, the spectrum has been identified as corresponding to the anion-radical $StQ^{\cdot -}$. Its carbon-centered mesomeric form is apparently responsible for formation of the aldehyde product via double bond cleavage (vide infra). In $StQ^{\cdot -}$ ($g = 2.00354$), there are 2 equivalent phenyl rings with two equivalent *m*-protons each ($a(4H) = 1.47$ G). An interesting case of non-equivalence is observed for the ethenyl protons ($a(1H) = 6.44$ G and $a(1H) = 2.78$ G), which is probably due to solvation effects or steric reasons.

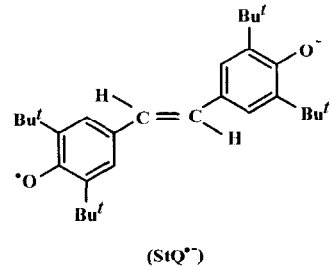

Anion-radical $StQ^{\cdot -}$ can also be detected when an equimolar mixture of H_2StQ and StQ is warmed to about 50°C under nitrogen in benzene solution. In this case it is formed due to

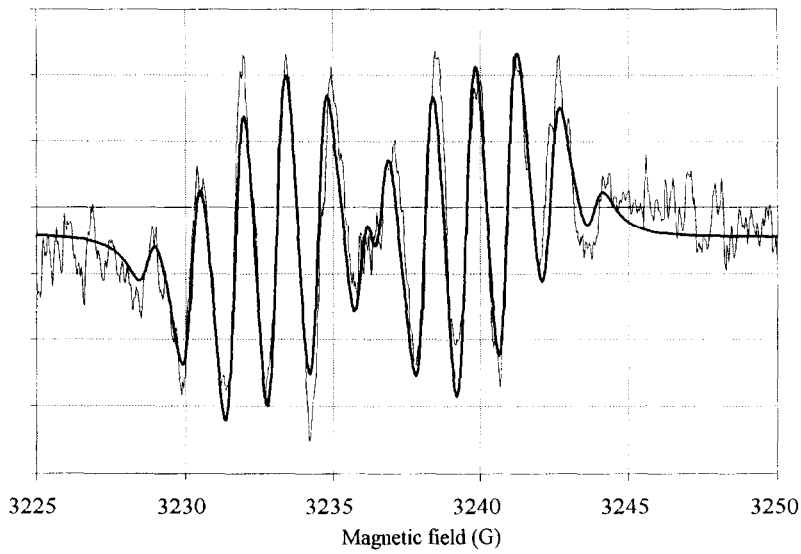

Fig. 3. ESR spectrum of the anion-radical intermediate $StQ^{\cdot -}$. The thin line is the experimental spectrum; the thick line has been simulated with $g = 2.00354$; $a(1H) = 6.44$ G; $a(1H) = 2.78$ G; $a(4H) = 1.47$ G.

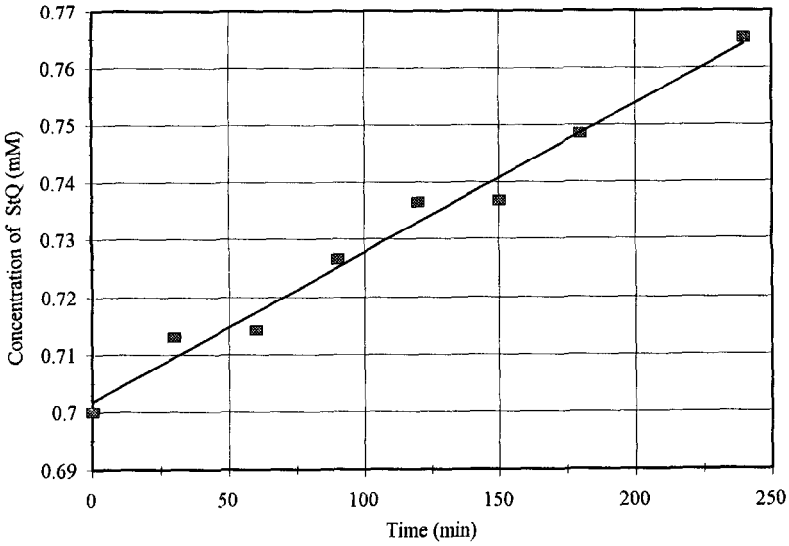

Fig. 4. Autoxidation of H_2StQ in air monitored by HPLC. $[H_2StQ]_0 = 6.87 \times 10^{-4}$ M; $[StQ]_0 = 7.00 \times 10^{-4}$ M; in benzene at $T = 323$ K.

electron transfer from H_2StQ to StQ and subsequent deprotonation. The same mixture in an oxygen atmosphere leads to the autoxidation of H_2StQ to StQ, as shown by HPLC analysis (Fig. 4).

The formation of $StQ^{\cdot -}$ as an intermediate demonstrates that the StQ product is formed from H_2StQ via 2-step oxidative dehydrogenation mediated by the cobaloxime(II) catalyst. However, no H_2O_2 was detected as an intermediate or product in the reaction.

3.3. Kinetic measurements

O_2-absorption curves were recorded in a constant pressure gas-volumetric apparatus as a

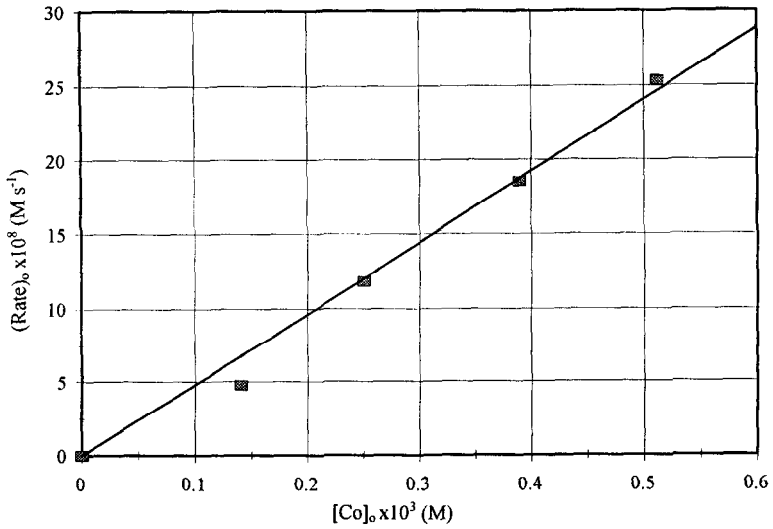

Fig. 5. Initial rate of O_2 absorption as a function of cobaloxime(II) concentration. $[H_2StQ]_0 = 5.95 \times 10^{-3}$ M; $P(O_2) = 630$ Torr; $T = 298$ K; solvent: benzene.

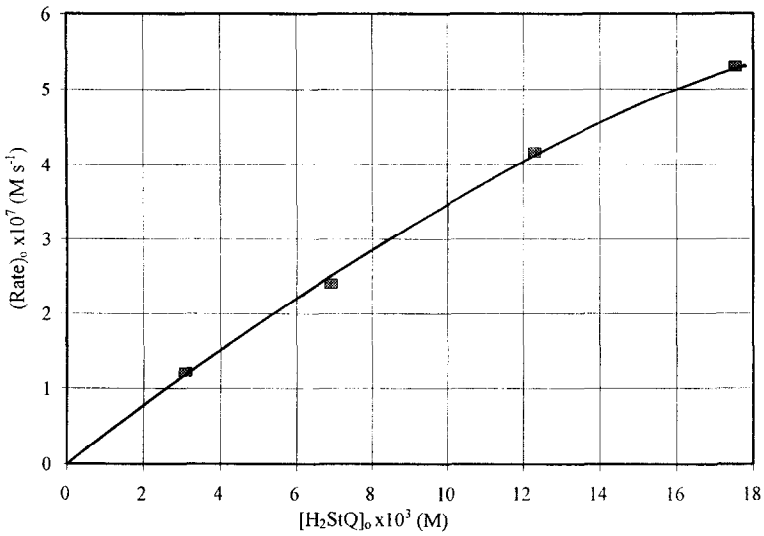

Fig. 6. Initial rate of O_2 absorption as a function of H_2StQ concentration. $[Co]_0 = 0.39 \times 10^{-3}$ M; $P(O_2) = 630$ Torr; $T = 298$ K; solvent: benzene.

function of cobaloxime(II) and H_2StQ concentration, and the partial pressure of dioxygen, i.e. its concentration. The initial rates of O_2 absorption (v_0) determined from these curves were used for elucidating the kinetics of the reaction. Unless otherwise specified, 'rate' refers to the initial rate of O_2 absorption.

Figs. 5 and 6 show the dependence of the initial rate on the catalyst and substrate concentration, respectively. The variation of the rate on dioxygen pressure is shown in Fig. 7.

Plots of the reciprocal rate ($1/v_0$) against the reciprocal H_2StQ concentration (Fig. 8) and reciprocal O_2 concentration (Fig. 9) gave excellent straight lines.

With reference to earlier results on cobaloxime(II)-catalyzed oxidations [21,22], the observed kinetic behavior is consistent with the

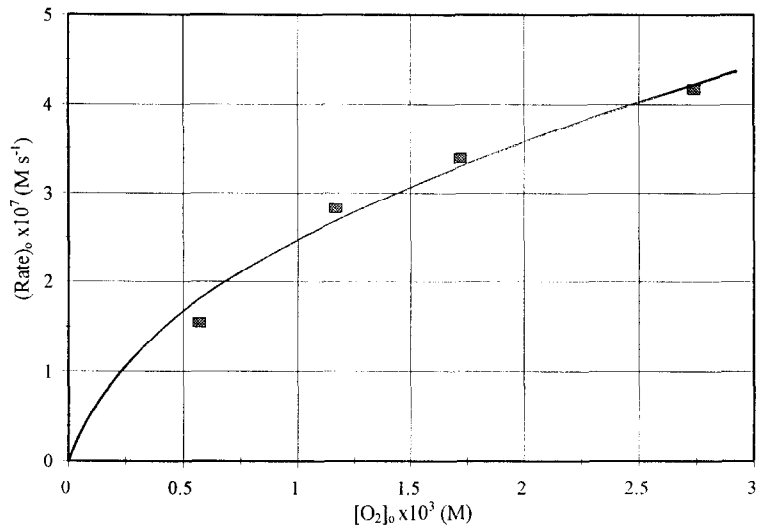

Fig. 7. Initial rate of O_2 absorption as a function of O_2 concentration. $[Co]_0 = 0.40 \times 10^{-3}$ M; $[H_2StQ]_0 = 12.3 \times 10^{-3}$; $T = 298$ K; solvent: benzene.

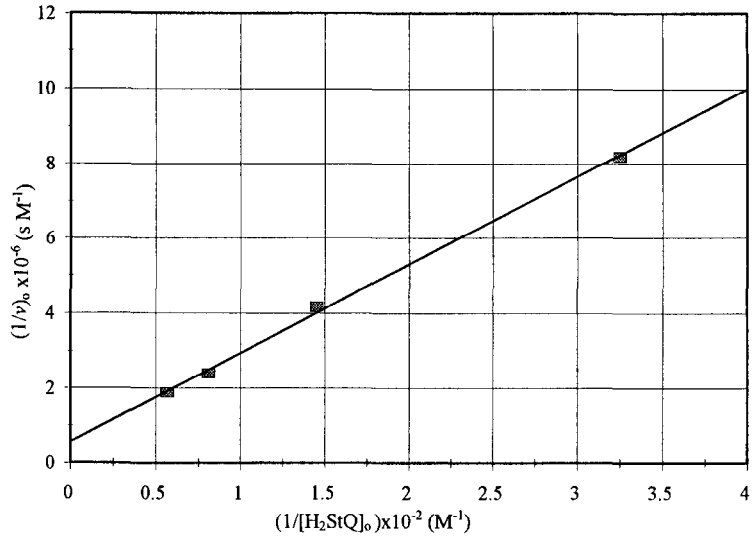

Fig. 8. Plot of reciprocal initial rate of O_2-absorption against $1/[H_2StQ]$. Conditions as in Fig. 6.

reaction mechanism (1)–(8), where Co^{II} and Co^{III} represent the $[Co^{II}(Hdmg)_2(Ph_3P)]$ and $[Co^{III}(Hdmg)_2(Ph_3P)]^+$ moiety, respectively:

$$Co^{II} + O_2 \rightleftarrows Co^{III}O_2 \quad \text{(pre-equil.)} \qquad (1)$$

$$Co^{III}O_2 + H_2StQ \rightleftarrows X \quad \text{(pre-equil.)} \qquad (2)$$

$$X \rightarrow Co^{III}O_2H + StQ^{\cdot -} + H^+ \quad \text{(slow)} \qquad (3)$$

$$2Co^{III}O_2H \rightarrow 2Co^{III}OH + O_2 \quad \text{(fast)} \qquad (4)$$

$$Co^{III}OH + StQ^{\cdot -} \rightarrow Co^{II} + StQ + OH^- \quad \text{(fast)} \qquad (5)$$

$$Co^{III}O_2 + StQ^{\cdot -} \rightarrow CoOOR^- \quad \text{(fast)} \qquad (6)$$

$$CoOOR^- + 2H^+ \rightarrow 2Ald + (Co^{III})^+ \qquad (7)$$

$$(Co^{III})^+ + OH^- \rightarrow Co^{III}OH \quad \text{(fast)} \qquad (8)$$

The rate law corresponding to the proposed mechanism can be derived by assuming that

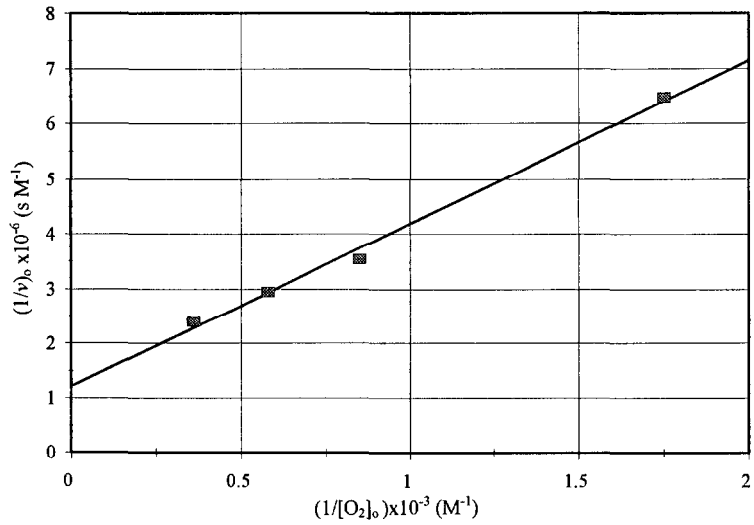

Fig. 9. Plot of reciprocal initial rate of O_2-absorption against $1/[O_2]$. Conditions as in Fig. 7.

steps (1) and (2) are reversible and step (3) is rate-determining. Disproportionation (4) can be regarded as fast [38], consequently, the concentration of $Co^{III}O_2H$ is negligible. As we are dealing with initial rates and the formation of Ald is delayed relative to that of StQ, steps (6) and (7) can be disregarded and the concentration of $CoOOR^-$ is also negligible. The balance equation (9) can thus be simplified to (10):

$$[Co]_0 = [Co^{II}] + [Co^{III}O_2] + [Co^{III}OH] + [X] + [Co^{III}O_2H] + [CoOOR^-] \quad (9)$$

$$[Co]_0 = [Co^{II}] + [Co^{III}O_2] + [Co^{III}OH] + [X] \quad (10)$$

The concentration of X expressed from Eq. (10) using the equilibrium constants K_1 and K_2 can be inserted into the rate equation for step (3), affording kinetic Eq. (11):

$$v = k_3[X] = k_3([Co]_0 - [Co^{III}OH]) \times \frac{K_1K_2[O_2][H_2StQ]}{1 + K_1[O_2](1 + K_2[H_2StQ])} \quad (11)$$

As we have measured initial rates (v_0), we can further simplify kinetic Eq. (11) by considering that at $t \approx 0$, $[Co^{III}OH] \approx 0$. Therefore:

$$v_0 \approx k_3[Co]_0 \frac{K_1K_2[O_2][H_2StQ]}{1 + K_1[O_2](1 + K_2[H_2StQ])} \quad (12)$$

The observed kinetic behavior is consistent with the rate law (12) as demonstrated by the data in Figs. 5–9. The linear plots of Figs. 8 and 9 yield the rate and equilibrium constants listed in Table 2 together with the sources and ways of calculation. Good agreement is found between values of K_2 obtained from different sources. For the calculations the solubility of dioxygen in benzene has been measured; it was found that $[O_2] = (3.26 \pm 0.15) \times 10^{-3}$ M at a dioxygen partial pressure of 650 Torr. The values given in Table 2 were used to compare the experimental and calculated slopes of the v_0 versus $[Co]_0$ plot. The experimental slope of 4.83×10^{-4} s^{-1} is in good agreement with the calculated value of 5.04×10^{-4} s^{-1}.

Mechanism (1)–(8) is analogous to the one proposed for the cobaloxime(II)-catalyzed oxidation of 2-aminophenol [21] and 3,5-di-*tert*-butylcatechol [22]. The active species is the superoxocobaloxime, $Co^{III}O_2$, which abstracts an H-atom from the substrate H_2StQ via an H-bonded intermediate X, affording the anion-radical detected ($StQ^{\cdot -}$). Intermediate X is necessary because of the requirement of an equilibrium involving H_2StQ (to account for the deviation from first-order behavior). The second oxidation (electron transfer) step occurs between $StQ^{\cdot -}$ and $Co^{III}OH$, which is formed via the known disproportionation of $Co^{III}O_2H$ with regeneration of one half of the amount of O_2 bound in the superoxocobaloxime $Co^{III}O_2$.

Formation of the aldehyde product requires

Table 2
Rate and equilibrium constants

No.	Source [a]	k_3 (s^{-1})	K_1 (M^{-1})	K_2 (M^{-1})
1	$(intercept)_2$	$(4.42 \pm 0.32) \times 10^{-3}$		
2	$(slope)_2/(slope)_1$		$(2.81 \pm 0.21) \times 10^2$	
3	$(intercept)_1/(slope)_2$			36.0
4	$(slope)_1$			55.0
5	$(slope)_2$			56.0
6	$(intercept)_1$			70.0
	average (rows 3–6)			54.0 ± 14

[a] Subscripts 1 and 2 refer to the $1/v$ versus $1/[O_2]$ and $1/v$ versus $1/[H_2StQ]$ plots, respectively.

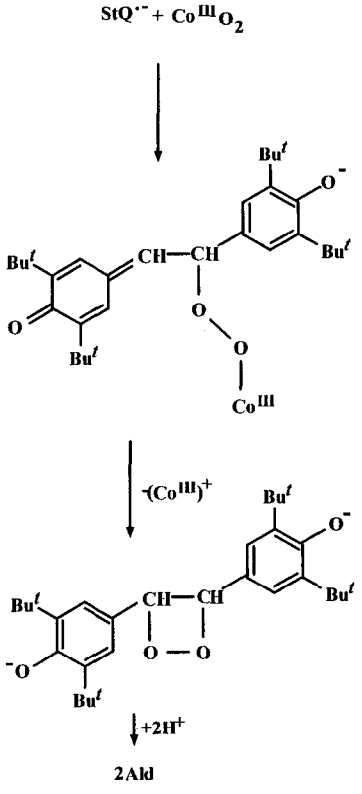

Scheme 2.

the presence of the cobaloxime(II) catalyst (Ald is not produced in the noncatalytic $H_2StQ/StQ/O_2$ system). This indicates a reaction between $Co^{III}O_2$ and $StQ^{\cdot -}$ in which the latter is attacked in its mesomeric form with the unpaired electron at one of the olefinic carbon atoms. The alkylperoxocobaloxime(III) formed is derived from the water present in ordinary benzene. The reduction equivalent required for generating the OH group in the second Ald molecule is provided by the $Co^{II} \rightarrow Co^{III}$ transformation: Co^{II} enters the cycle in step (1) and $(Co^{III})^+$ is produced in step (7). The proposed reaction mechanism is depicted in Scheme 2.

In conclusion the substrate H_2StQ has proved to be a useful diagnostic tool for characterizing the ability of the cobaloxime(II)/O_2 catalyst system to abstract an H-atom (or an electron and H^+) from suitable reactants. Also, it has been possible for the first time to show that this catalyst is capable of effecting the oxidative cleavage of an olefinic double bond. This propensity is also closely related to the formation of free radicals, which ensure that the O–O moiety can be catalytically attached to a carbon atom. Former examples of cobaloxime catalyzed oxidations invariably involve substrates with reactive H-atoms (OH or NH) and they are in fact to be regarded as oxidative dehydrogenations, rather than oxygen insertions. It is now conceivable that the cobaloxime system shows certain features also exhibited by dioxygenase enzymes, and this can be utilized in biomimetic studies.

It will be of interest to search for further examples of this type of behavior.

Acknowledgements

This work was supported by the Hungarian Research Fund (OTKA Grant T 015830) and by COST Chemistry Action D1 (PECO 12984).

References

[1] L.I. Simándi, Catalytic Activation of Dioxygen by Metal Complexes (Kluwer Academic Publishers, Dordrecht, 1992).
[2] L.I. Simándi (Ed.), Dioxygen Activation and Homogeneous Catalytic Oxidation, Studies in Surface Science and Catalysis, Vol. 66 (Elsevier Science Publishers, Amsterdam, 1991).
[3] L.I. Simándi, Int. Rev. Phys. Chem. 8 (1989) 21.
[4] D.H.R. Barton, A.E. Martell and D.T. Sawyer (Eds.), The Activation of Dioxygen and Homogeneous Catalytic Oxidation (Plenum Press, New York, 1993).
[5] J. Reedijk (Ed.), Bioinorganic Catalysis (Marcel Dekker, New York, 1993).
[6] E.-I. Ochiai, in: Metal Ions in Biological Systems, H. Sigel and A. Sigel (Eds.), Vol. 30 (Marcel Dekker, New York, 1994) pp. 1–24.
[7] E. Tsuchida and K. Yamamoto, in: Bioinorganic Catalysis, J. Reedijk (Ed.) (Marcel Dekker, New York, 1993) pp. 29–87.
[8] J.M. Whittaker, in: Metal Ions in Biological Systems, H. Sigel and A. Sigel (Eds.), Vol. 30 (Marcel Dekker, New York, 1994) pp. 315–403.
[9] N. Ito, S.E.V. Phillips, C. Stevens, Z.B. Ogel, M.J. McPherson, J.K. Keen, K.D.S. Yadav and P.F. Knowles, Nature 350 (1991) 87.
[10] K.Y. Lam, D.G. Fortier and A.G. Sykes, J. Chem. Soc. Chem. Commun. (1990) 1019.
[11] S. Németh and L.I. Simándi, J. Mol. Catal. 14 (1982) 87.

[12] S. Németh and L.I. Simándi, J. Mol. Catal. 14 (1982) 241.
[13] S. Németh and L.I. Simándi, J. Mol. Catal. 22 (1984) 341.
[14] L.I. Simándi, S. Németh and N. Rumelis, J. Mol. Catal. 42 (1987) 357.
[15] L.I. Simándi, A. Fülep-Poszmik and S. Németh, J. Mol. Catal. 48 (1988) 265.
[16] Z. Szeverényi and L.I. Simándi, J. Mol. Catal. 51 (1989) 155.
[17] Z. Szeverényi, E.R. Milaeva and L.I. Simándi, J. Mol. Catal. 67 (1991) 251.
[18] Z. Szeverényi, L.I. Simándi and R. Iwanejko, J. Mol. Catal. 64 (1991) L15.
[19] L.I. Simándi, T. Barna, Z. Szeverényi and S. Németh, Pure Appl. Chem. 64 (1992) 1511.
[20] L.I. Simándi, T. Barna, L. Korecz and A. Rockenbauer, Tetrahedron Lett. 34 (1993) 717.
[21] L.I. Simándi, T. Barna and S. Németh, J. Chem. Soc. Dalton Trans. (1996) 473.
[22] L.I. Simándi, T. Barna, Gy. Argay and T.L. Simándi, Inorg. Chem. 34 (1995) 6337.
[23] T.L. Simándi, A. Rockenbauer and L.I. Simándi, Eur. Polym. J. 31 (1995) 555.
[24] J.N. Abelson and M.I. Simon (Eds. in Chief), Methods in Enzymology, Biomass, Part B, Lignin, Pectin and Chitin, W.A. Wood and S.C. Kellogg (Eds.), Vol. 161 (Academic Press, New York, 1988).
[25] D. Dolphin, in: The Activation of Dioxygen and Homogeneous Catalytic Oxidation, D.H.R. Barton, A.E. Martell and D.T. Sawyer (Eds.) (Plenum Press, New York, 1993) p. 287.
[26] G. Labat and B. Meunier, Bull. Soc. Chim. Fr. 127 (1990) 553.
[27] J. Giererand and N.-O. Nilvebrant, Holzforschung Suppl. 40 (1986) 107.
[28] D.E. Hamilton, R.S. Drago and J. Telser, J. Am. Chem. Soc. 106 (1984) 5353.
[29] R.S. Drago, B.B. Corden and C.W. Barnes, J. Am. Chem. Soc. 108 (1986) 2453.
[30] C.L. Bailey and R.S. Drago, Coord. Chem. Rev. 79 (1987) 321.
[31] P.A. Ganeshpure and S. Satish, Tetrahedron Lett. 29 (1988) 6629.
[32] A. Nishinaga, H. Iwasaki, T. Shimizu, Y. Toyoda and T. Matsuura, J. Org. Chem. 51 (1986) 2257.
[33] P.W. Schneider, P.F. Phelan and J. Halpern, J. Am. Chem. Soc. 91 (1969) 77.
[34] G.N. Schrauzer and L.P. Lee, J. Am. Chem. Soc. 92 (1970) 1551.
[35] A. Rockenbauer, É. Budó-Záhonyi and L.I. Simándi, J. Chem. Soc. Dalton Trans. (1975) 1729.
[36] E.S. Brownstein and K.U. Ingold, J. Am. Chem. Soc. 84 (1962) 2258.
[37] M.D. Wirt, C.J. Bender and J. Peisach, Inorg. Chem. 34 (1995) 1663.
[38] L.I. Simándi, C.R. Savage, Z.A. Schelly and S. Németh, Inorg. Chem. 21 (1982) 2765.